Ventral prostate and mammary gland phenotype in mice with complete deletion of the ERβ gene

Margaret Warner[a,1], Wan-fu Wu[a], Leticia Montanholi[b], Ivan Nalvarte[b], Per Antonson[b], and Jan-Ake Gustafsson[a,b,1]

[a]Center for Nuclear Receptors and Cell Signaling, Department of Biology and Biochemistry, University of Houston, Houston, TX 77204; and [b]Center for Innovative Medicine, Department of Biosciences and Nutrition, Karolinska Institutet, Novum, 14186 Stockholm, Sweden

Disagreements about the phenotype of estrogen receptor β (ERβ) knockout mouse, created by removing the DNA-binding domain of the ERβ gene or interruption of the gene with a neocassette (Oliver Smithies ERβ knockout mice [ERβ$^{OS-/-}$]), prompted us to create an ERβ knockout mouse by deleting the ERβ gene with the use of CRISPR/Cas9 technology. We confirmed that the ERβ gene was eliminated from the mouse genome and that no ERβ mRNA or protein was detectable in tissues of this mouse. Overall the phenotype of the ventral prostate (VP) and mammary gland (MG) in ERβ$^{crispr-/-}$ mice was similar to, but more severe than, that in the ERβ$^{OS-/-}$ mice. In the VP of 6-mo-old ERβ$^{crispr-/-}$ mice there was epithelial hyperplasia, fibroplasia, inflammation, stromal overgrowth, and intraductal cancer-like lesions. This was accompanied by an increase in Ki67 and P63 and loss in DACH1 and PURα, two androgen receptor (AR) repressors. In the MG there was overexpression of estrogen receptor α and progesterone receptor, loss of collagen, increase in proliferation and expression of metalloproteases, and invasive epithelium. Surprisingly, by 18 mo of age, the number of hyperplastic foci was reduced, the ducts of the VP and MG became atrophic, and, in the VP, there was massive immune infiltration and massive desquamation of the luminal epithelial cells. These changes were coincident with reduced levels of androgens in males and estrogens in females. We conclude that ERβ is a tumor suppressor gene in the VP and MG where its loss increases the activity AR and ERα, respectively.

CRISPR | fibroplasia | chemokine

Since its discovery in 1996 (1), the physiological role of ERβ has been under intense scrutiny. Some aspects of ERβ signaling, which raised questions about whether it has a physiological function, are its weak affinity estrogen response elements (ERE), its lack of effect on the pituitary and uterus, and disagreements over the phenotype of the knockout mice, which were created in different laboratories (2–6). In addition, the use of less than optimal antibodies has resulted in some erroneous conclusions about localization of ERβ (7).

We now know that ERβ exerts most of it effects through tethering to other transcription factors and not by binding to ERE (8, 9) and, except for reduced ovulation, the removal of the DNA-binding domain (DBD) had little effect on the physiological functions of ERβ (2, 5). All laboratories studying ERβ knockout mice agreed that ovulation was severely compromised whether the gene was interrupted by a neocassette (ERβ$^{OS-/-}$) or the DBD was removed. Thus, there is a clear role for ERβ in ovulation. This role is likely due to effects of ERβ on gonadotropin-releasing hormone (GnRH) signaling (6) and not to change in the ovary itself (10, 11). Without the GnRH release at mid cycle, there would be no luteinizing hormone (LH) surge and no ovulation. What this means is that ERβ is essential for survival of the species because without it female reproduction would be severely compromised. The lack of ERβ expression in the pituitary and uterus is now considered advantageous because ERβ agonists may be used in men and women without causing chemical castration or uterine growth.

Although ERβ was originally cloned from a prostate cDNA library, the most controversial issue in the different ERβ ko mice is whether there is a phenotype in the ventral prostate (VP) (2, 12). Comparison of the transcripts (by RNA sequencing) of wild-type (WT) and ERβ$^{OS-/-}$ mouse VP showed that genes involved in prostate cancer (PCa) were increased upon inactivation of ERβ (5). Despite its regulation of genes associated with PCa, ERβ$^{OS-/-}$ mice do not develop PCa. Mak et al. have suggested that in PCa, the event causing malignancy has already occurred before loss of ERβ. Thus, ERβ loss contributes to the progress of PCa but loss of ERβ itself does not cause malignancy (13).

From a clinical perspective, the possibility that ERβ opposes the action of the androgen receptor (AR) suggests a novel approach to treatment of PCa, which is an androgen receptor-driven disease. Very effective ERβ agonists have been synthesized (14, 15) and found to be very safe drugs (16).

In the mammary gland (MG) of ERβ$^{OS-/-}$ mice, the epithelium was not fully differentiated (17): Levels of the adhesion molecules, E-cadherin, connexin 32, occludin, and integrin α were reduced and no zonula occludens was detectable. In the present study of the ERβ$^{crispr-/-}$ mouse MG, there was overexpression of ERα and invasive epithelium. The MG and VP of ERβ$^{crispr-/-}$ mice have confirmed a key role for ERβ in controlling growth and differentiation of the epithelium of both of these organs.

Results

Loss of ERβ Transcripts in the ERβ$^{crispr-/-}$ Mice. A mouse line with a constitutive knock-out of the ERβ gene was made using CRISPR/Cas9-mediated gene editing (Fig. 1A). All 10 exons of the ERβ

Significance

The discovery of ERβ caused a new optimism for understanding and treatment of prostate cancer. However, over the past 20 y, many mistakes have been made in studies trying to define the physiological functions of ERβ. One of the bigger problems has been producing a good ERβ knockout mouse. Deletion of the DNA-binding domain of ERβ did not produce a knockout of ERβ function because most functions of ERβ do not rely on DNA binding of the receptor. We have now deleted the entire ERβ gene from the mouse genome and report that ERβ regulates growth and differentiation of the ventral prostate and mammary gland.

Fig. 1. Confirmation of loss of ERβ expression in the mammary gland and ventral prostate. (A) Knockout of the ERβ gene with the use of CRISPR/Cas9-mediated gene editing. qPCR of mRNA from the ovary (B) and immunohistochemical staining for ERβ in the mammary gland (C and D) and ventral prostate (E and F) of WT and ERβ$^{crispr-/-}$ mouse. There is no detectable ERβ mRNA in the ovaries, and ERβ protein is expressed in the epithelium (red arrow) and stroma (black arrow) of WT mice, but there is no detectable expression in the ERβ$^{crispr-/-}$ mouse. The antibody used was the IgY antibody raised against ERβ protein lacking the amino acids at the N terminal of the protein. (Scale bars: 50 μm.)

gene were deleted by using two single guide RNA (sgRNA) that bind 1.3 kb upstream of exon 1 and 0.6 kb downstream of exon 10, respectively. These sgRNAs caused a 59-kb deletion, including all ERβ exons and the proximal promoter, after CAS9-mediated genome editing in zygotes. The sgRNAs used were selected for a low number of predicted off-targets, and the founder mice have been back-crossed three times to further reduce the risk of off-target mutations.

qRT-PCR and immunohistochemistry confirmed that there was a complete loss of the ERβ RNA in the ovaries of the mouse (Fig. 1B) and a complete loss of the ERβ protein from the mammary gland and ventral prostate (Fig. 1 C–F).

**Epithelial Hyperplasia and Intraductal Cancer-Like Lesions in ERβ$^{crispr-/-}$ Mouse.** At 6 mo of age, in the ERβ$^{crispr-/-}$ mouse, many foci of epithelial hyperplasia (Fig. 2 C and D) and intraductal cancer-like lesions (Fig. 2 E and F) were found. Epithelial cell polarization was lost. At this age the number of cells expressing the proliferation marker (Ki67) (Fig. 3 A, C, and E) and the basal cell marker (P63)

(Fig. 3 B, D, and F) was markedly increased. There was a decrease in the expression of DACH1 (the androgen receptor repressor) and an increase in RORc (the driver of AR) (*SI Appendix*, Fig. S1). Epithelial hyperplasia was also found in 13-mo-old ERβ$^{crispr-/-}$ mouse VP (Fig. 2 G and H) with increased Ki67-positive cells and P63-positive cells (*SI Appendix*, Fig. S2). However, in 18-mo-old ERβ$^{crispr-/-}$ mouse, VP epithelial hyperplasia was markedly reduced (Fig. 2 I and J).

Fibroplasia in ERβ$^{crispr-/-}$ Mouse. Fibroplasia was found at all ages of ERβ$^{crispr-/-}$ mouse VP. In 6-mo-old ERβ$^{crispr-/-}$ mouse, VP
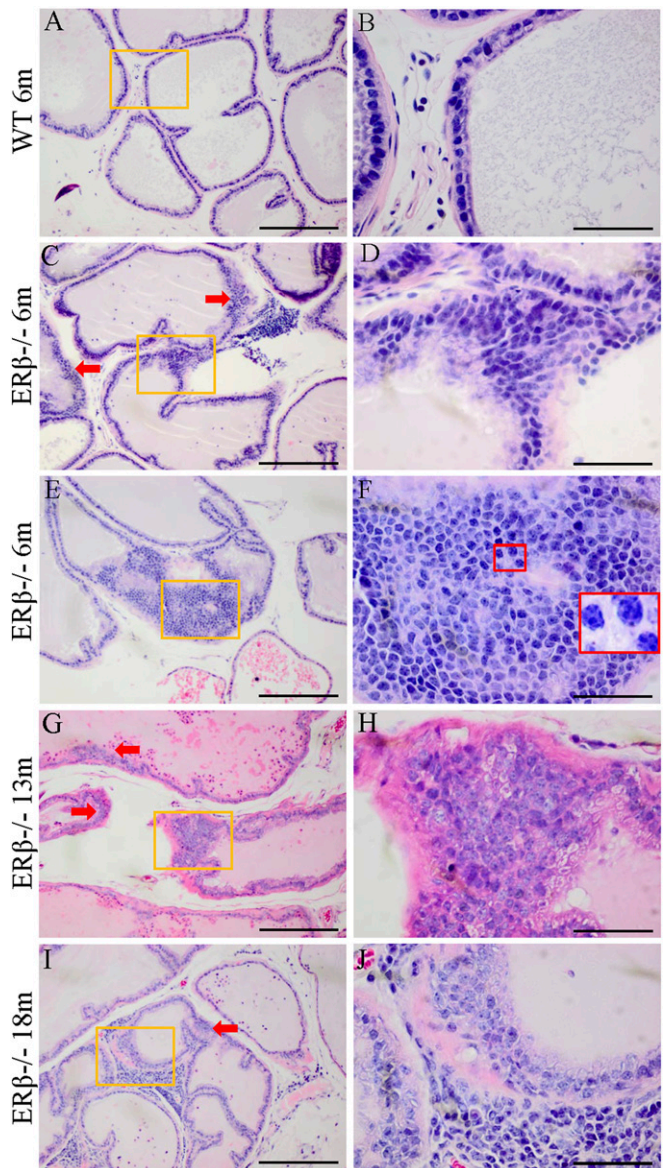
Fig. 2. Epithelial hyperplasia and in situ ductal cancer-like lesion in ERβ$^{crispr-/-}$ mouse VP. (A and B) HE staining of 6-mo-old WT mouse ventral prostate. There are many foci of epithelial hyperplasia (C and D) and in situ ductal cancer-like lesion (E and F) in 6-mo-old ERβ$^{crispr-/-}$ mouse VP. (F, Inset) High magnification picture shows abnormal nucleoli. The epithelial cells appear to have lost polarity. (E and F) Reprinted from ref. 7. Copyright (2019), with permission from Elsevier. (G and H) Epithelial hyperplasia was also found in 13-mo-old ERβ$^{crispr-/-}$ mouse VP. (I and J) However, in 18-mo-old ERβ$^{crispr-/-}$ mouse VP epithelial hyperplasia was reduced. Red arrows indicate epithelial hyperplasia. (Scale bars: A, C, E, G, and I, 200 μm; B, D, F, H, and J, 50 μm.)

MEDICAL SCIENCES
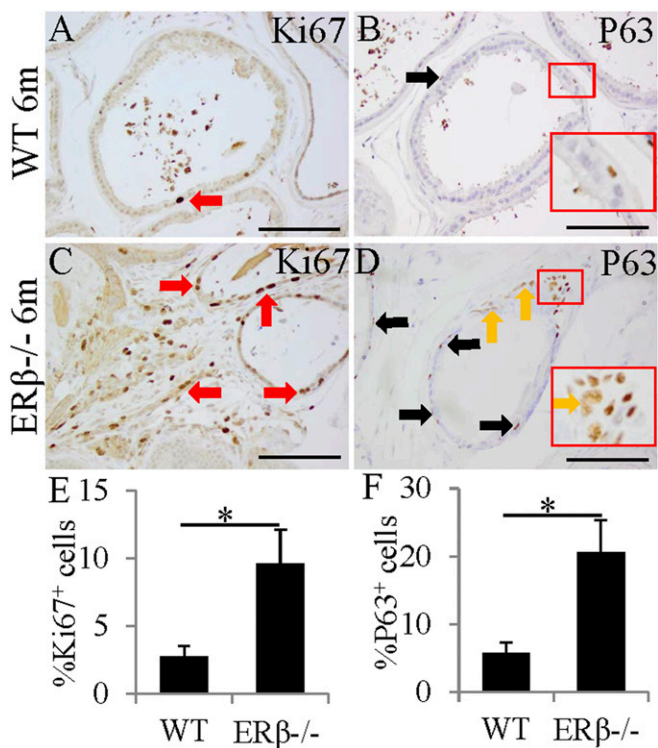
Fig. 3. Increased Ki67-positive cells and P63-positive cells in VP of ERβ−/− mice. (*A* and *B*) A few Ki67-positive cells and P63-positive cells were identified in VP of WT mice. In ERβ^crispr−/− mice, there were many more Ki67-positive cells and P63-positive cells than in VP of WT mice. (*C* and *D*) In addition to cells in basal layer, some cells in luminal cell layer are P63-positive (orange arrows). (*E* and *F*) In ERβ^crispr−/− mouse VP, the number of Ki67-positive cells and p63-positive cells was 3.3-fold higher and 3.1-fold higher, respectively (*$P <$ 0.05). Red arrows indicate Ki67-positive cells, and black arrows indicate P63-positive cells. (Scale bars: 100 μm.)

fibroplasia was found within the ducts (Fig. 4 *C* and *D*). At 13 mo of age, in the ERβ crispr−/− mouse, macrophages, identified by Iba1 staining (Fig. 4 *F*, *Inset*), filled those ducts where there was fibroplasia (Fig. 4 *E* and *F*). The fibroplasia remained in 18-mo-old ERβ^crispr−/− mouse VP within enlarged ducts filled with dying epithelial cells (Fig. 4 *G* and *H*).

Immune Cell Invasion in ERβ^crispr−/− Mouse. Mild immune cell invasion was found in 18-mo-old WT mouse VP (Fig. 5 *A* and *B*). In 6-mo-old ERβ^crispr−/− mouse VP, there was no obvious invasion of immune cells although there were foci of epithelial hyperplasia and fibroplasia (Fig. 5 *C* and *D*). In 13-mo-old ERβ^crispr−/− mouse VP, there was immune-cell invasion (Fig. 5 *E* and *F*). At 18 mo of age, massive immune cell invasion was found in VP (Fig. 5 *G* and *H*).

Desquamation in ERβ^crispr−/− Mouse. There was no obvious desquamation of luminal epithelial cells into the ducts in 18-mo-old WT mouse VP (Fig. 6 *A* and *B*) or 6-mo-old ERβ^crispr−/− mouse VP (Fig. 6 *C* and *D*). There was substantial desquamation in ducts of 13-mo-old ERβ^crispr−/− mouse VP, and there were regions of the ducts where there were no epithelial cells (Fig. 6 *E* and *F*). In some ducts, the desquamation was so severe that it resembled those of men undergoing androgen deprivation therapy (ADT) (18).

To understand the marked change in the VP with age, we measured androgen levels in males and estrogen levels in females in mice of 7, 13, and 18 mo of age. Serum levels of estradiol and androgen were measured in a single run by gas chromatography-tandem mass spectrometry (GC-MS/MS). We found a marked

reduction in testosterone levels in both WT (2,948 ± 2,158 pg/mL) and ERβ−/− mice (3,316 ± 2,025 pg/mL) in 18-mo-old mice. In young intact males T levels are 8,235 ± 1,055 pg/mL. It therefore appears that, with age, both WT and ERβ^crispr−/− become androgen-deficient, and this leads to loss of androgen-induced prostatic hyperplasia.

In order to confirm that the reduced levels of androgen did have consequences on androgen signaling, expression of prostatic acid phosphatase (PAP) and probasin, two AR regulated genes, was examined in 8-mo-old and 18-mo-old ERβ crispr−/− mouse. PAP and probasin were both higher in 8-mo-old ERβ crispr−/− mouse than in their WT littermates, indicating an increase in androgen signaling (*SI Appendix*, Fig. S3 *A–D*). However, PAP and probasin were sharply decreased in 18-mo-old ERβ^crispr−/− and WT mice. (*SI Appendix*, Fig. S3 *E–H*). These results confirm that there is an increased AR signaling in young ERβ^crispr−/− mice but a loss of AR signaling in aging ERβ^crispr−/− and WT mouse VP.

Microarray Analysis of the VP. We compared the gene expression profile in the VP of 13-mo-old WT and ERβ^crispr−/− mice. There was an overwhelming predominance of immune genes in the ERβ^crispr−/− VP. These were mostly Ig kappa chains. When these
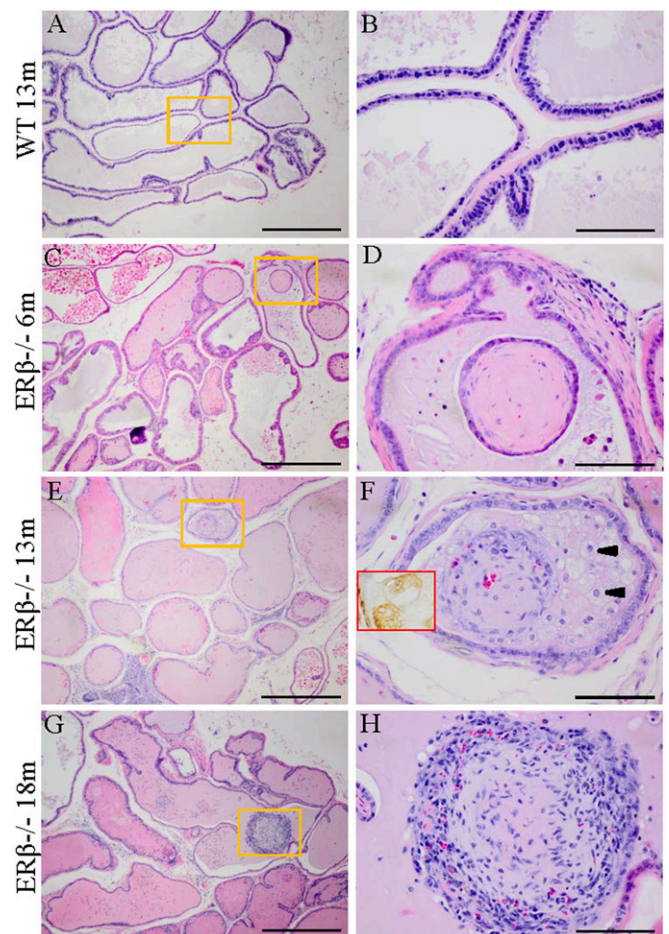
Fig. 4. Fibroplasia in ERβ^crispr−/− mouse VP. (*A* and *B*) HE staining of 13-mo-old WT mouse ventral prostate. (*C* and *D*) Fibroplasia was found in 6-mo-old ERβ^crispr−/− mouse VP. (*E* and *F*) Fibroplasia with macrophages within the duct was common in 13-mo-old ERβ^crispr−/− mouse VP. (*F*, *Inset*) Stained for Iba1 (a marker for macrophages) within duct. (*G* and *H*) In 18-mo-old ERβ^crispr−/− mouse VP, there were large fibroplastic lesions found within enlarged ducts along with dying epithelial cells. Black arrowheads indicate macrophages within duct. (Scale bars: *A*, *C*, *E*, and *G*, 500 μm; *B*, *D*, *F*, and *H*, 100 μm.)
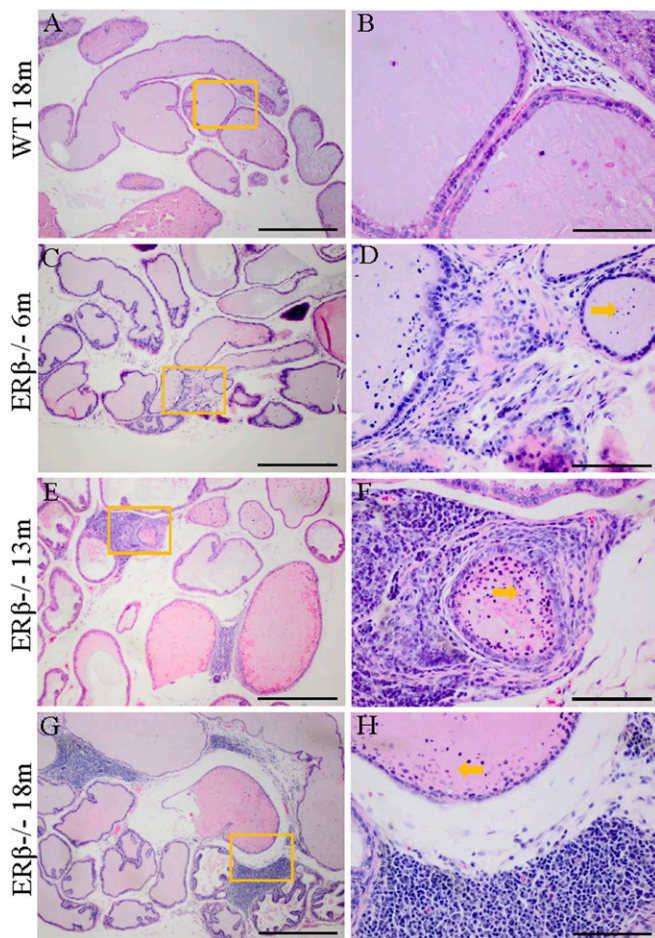
Fig. 5. Immune cell invasion in ERβ$^{crispr-/-}$ mouse VP. (*A* and *B*) A few immune cells were found in 18-mo-old WT mouse ventral prostate. (*C* and *D*) No obvious immune cell invasion was found in 6-mo-old ERβ$^{crispr-/-}$ mouse VP. (*E* and *F*) In 13-mo-old ERβ$^{crispr-/-}$ mouse VP, immune cell invasion was found. (*G* and *H*) Massive immune cell invasion was found in 18-mo-old ERβ$^{crispr-/-}$ mouse VP. Orange arrows indicate dying epithelial cells. (Scale bars: *A*, *C*, *E*, and *G*, 500 μm; *B*, *D*, *F*, and *H*, 100 μm.)

genes were filtered out, we were left with a set of genes (Table 1), several of which have been previously shown to be ERβ regulated (19).

One More ERβ-Regulated Gene Involved in Repression of Androgen Signaling. PURα (purine response binding transcriptional suppressor) is a novel suppressor of AR. It binds to purine response elements in the AR promoter and inhibits AR transcriptional activity (20, 21). PURα is a key repressor of AR transcription and its loss from the transcriptional repressor complex causes AR overexpression and progression of PCa to androgen-independent PCa. We found that PURα is an ERβ-induced gene. Its expression level is increased by ERβ agonists in 2-mo-old (Fig. 7 *A*, *D*, and *G*) and 6-mo-old WT mice (Fig. 7 *B*, *E*, and *H*) and decreased in ERβ$^{crispr-/-}$ mice (Fig. 7 *C*, *F*, and *I*). PURα can be added to the list of ERβ-regulated genes that control AR signaling.

Phenotype of the MG in ERβ$^{crispr-/-}$ Mouse. In the MG of ERβ$^{crispr-/-}$ mice, expression of ERα, PR, and Ki67 was higher than in WT mice (Fig. 8 *A–F* and *J–L*). There were lesions where proliferating epithelial cells invaded the stroma with no ductal structure (Fig. 8 *G–I*) and a complete lack of fibroblasts and collagen (Fig. 9 *C* and *F*). In the ERβ$^{crispr-/-}$ mouse MG, there was obvious epithelial hyperplasia (Fig. 9*B*). The collagen layer

in the ducts was reduced, and what was left appeared to be fragmented (Fig. 8*E*). This destruction of collagen was correlated with an increase in the level of MMPs in the mammary gland (Fig. 9 *H–S*).

As was the case in the prostate, the severe phenotype seen in the 6-mo-old mice was not evident in 18-mo-old mice. At this age the mammary ducts were atrophic, the ovary was devoid of follicles (*SI Appendix*, Fig. S4), and serum estradiol was below the level of detection.

Discussion

The present study has confirmed a key role for ERβ in controlling growth of the epithelium of the MG and VP. In both organs, ERβ represses the expression and transcriptional activity of the hormone which drives proliferation: In the VP, it opposes AR signaling and, in the MG, ERα expression and signaling. Along with reducing proliferation, ERβ regulates invasiveness of the epithelium by stimulating degradation of collagen and the extracellular matrix. In the MG these proteases are MMP9, 13, and 14. In the VP expression of the protease inhibitor WAP, four-disulfide core domain 3 (a secreted serine-type endopeptidase)
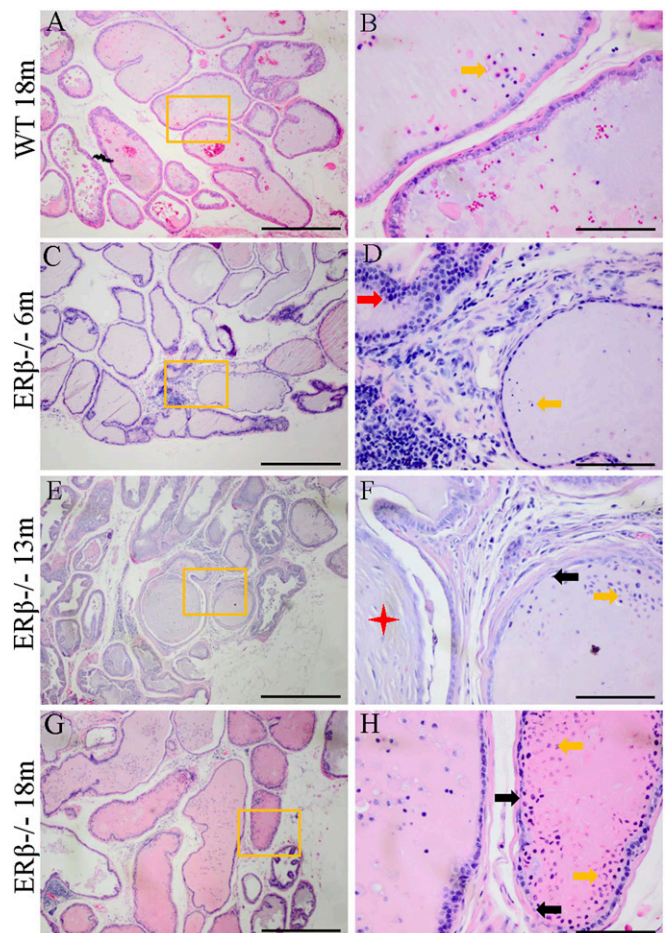
Fig. 6. Desquamation in ERβ$^{crispr-/-}$ mouse VP. (*A* and *B*) In 18-mo-old WT mouse ventral prostate, a few dying cells were found within ducts. (*C* and *D*) No obvious desquamation was seen in 6-mo-old ERβ$^{crispr-/-}$ mouse VP with epithelial hyperplasia. (*E* and *F*) In 13-mo-old ERβ$^{crispr-/-}$ mouse VP, desquamation was found and some regions of the ducts were devoid of epithelial cells. (*G* and *H*) There was much more desquamation in 18-mo-old ERβ$^{crispr-/-}$ mouse VP. Orange arrows indicate dying epithelial cells; Red star indicates fibroplasia; black arrows indicate places in the ducts where the epithelial cells have been lost. (Scale bars: *A*, *C*, *E*, and *G*, 500 μm; *B*, *D*, *F*, and *H*, 100 μm.)

Table 1. ERβ-regulated genes

| ANOVA $P < 0.05$	Fold change	Gene
0.005068	2.02	Alcohol dehydrogenase 6A
0.036602	1.98	Serum/glucocorticoid regulated kinase 1
0.028063	1.92	Sestrin1
0.006781	1.79	coagulation factor II (thrombin) receptor
0.020718	1.78	flavin containing monooxygenase 6
0.23392	1.69	glycerophosphodiester phosphodiesterase domain containing 2
0.03684	1.68	Grb2-binding adaptor, transmembrane
0.028829	1.63	small proline-rich protein 1A
0.043731	1.61	solute carrier family 6 (neurotransmitter transporter. Member 2
0.034154	1.59	sulfotransferase family 1E, member 1
0.03248	1.51	cyclin B2
0.007135	−1.5	FYVE and coiled-coil domain containing 1
0.041142	−1.45	PHD finger protein 1
0.047607	−1.54	guanine nucleotide binding protein (G protein), beta 5
0.012858	−1.57	phosphatidylethanolamine N-methyltransferase
0.026356	−1.58	leucine zipper and CTNNBIP1 domain containing
0.007209	−1.6	nuclear protein transcription regulator 1
0.020535	−1.894	pterin 4 alpha carbinolamine dehydratase/dimerization cofactor of hepatocyte nuclear factor 1 alpha (TCF1) 1
0.037626	−1.93	DDB1 and CUL4 associated factor 12-like 1
0.033728	−2.43	basic helix–loop–helix family, member a15
0.000936	−3.89	estrogen receptor 2 (beta)
0.005717	−5.72	WAP four-disulfide core domain 3

was markedly decreased. This gene, which has previously been identified as an ERβ-regulated gene (19), is secreted from prostate smooth muscle cells and functions as a growth inhibitor in the prostate (22). There was no invasive cancer in ERβ^crispr−/− mice. In fact, once the driving hormones were reduced in aging mice, the epithelial hyperplasia of both the VP and MG was reduced. Thus, in mice, ERβ is a tumor suppressor gene whose loss increases

signaling of AR and ERα but does not lead to invasive cancer. With age, as the levels of the driving hormones estradiol and androgen are decreased due to ovarian and testicular failure, there is less epithelial hyperplasia but the fibroplasia remains.

Fibroplasia is reactive stroma usually found in prostates with PCa. Barron et al. have produced fibroplasia in the mouse VP by overexpressing TGFβ under the control of an enhanced probasin
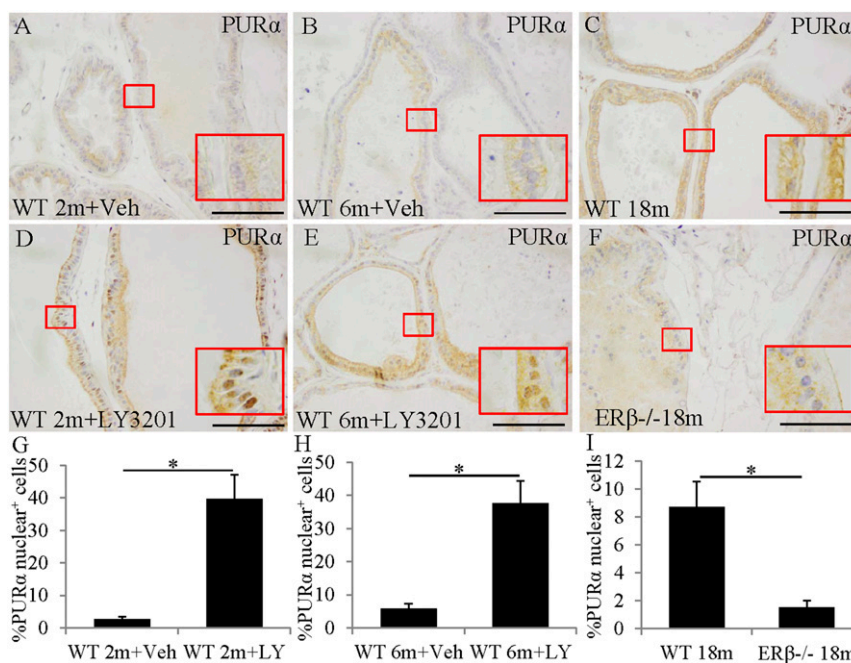
Fig. 7. Up-regulated PURα by ERβ agonist and down-regulated PURα expression in ERβ^crispr−/− mouse VP. Expression of PURα is increased by ERβ agonist in 2-mo-old (*A* and *D*) and 6-mo-old WT mice (*B* and *E*). (*G* and *H*) ERβ agonist significantly increased number of PURα-positive nuclei (*$P < 0.05$). PURα expression is markedly decreased in ERβ^crispr−/− mice (*$P < 0.05$) (*C*, *F*, and *I*). Insets are from high magnification. (Scale bars: *A–F*, 100 μm.)
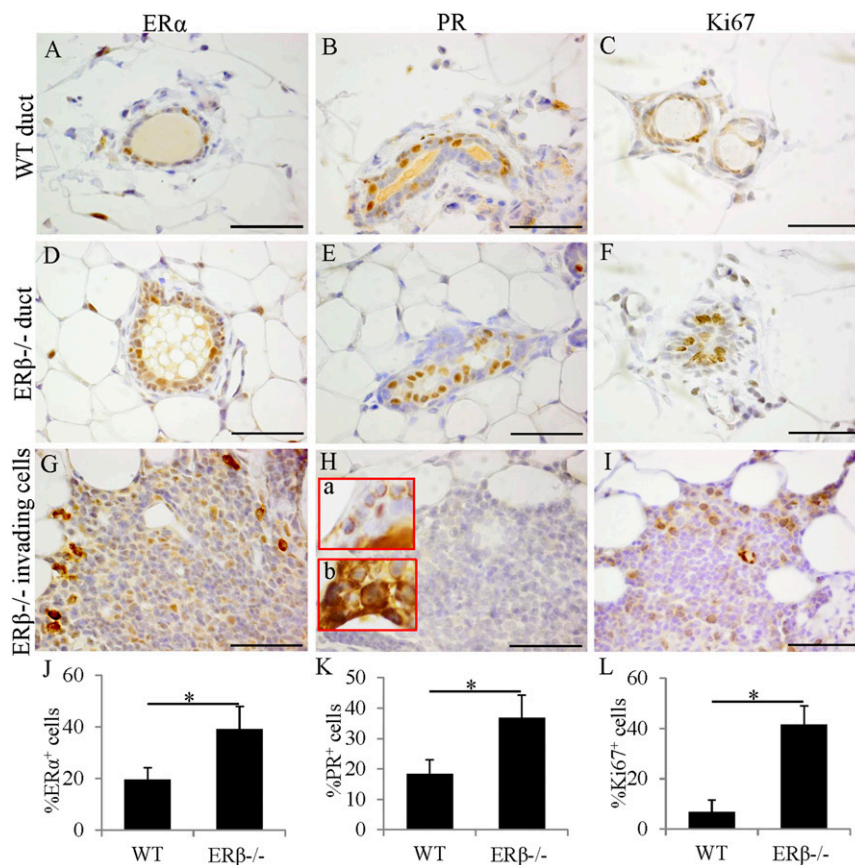
Fig. 8. Increased ERα, PR, and Ki67 expression in MG of 6-mo-old ERβ^crispr−/− female mouse. (*A–F*) Expression of ERα, PR, and Ki67 was higher than in WT mice. There were lesions where proliferating CK14-positive epithelial cells invaded the stroma. (*G–I*) These cells express ERα and Ki67. In *H*, *Insets*, *a* shows Ck14-positive myoepithelial cells and *b* shows Ck14-positive invading cells. Ck14-positive staining in invading cells demonstrates these cells are epithelial cells. (*J–L*) Statistical analysis of ERα, PR, or Ki67-positive cells in WT and ERβ^crispr−/− mice (*P < 0.05). (Scale bars: 50 μm.)

promoter and found lesions similar to those described here in the ERβ^crispr−/− mice (23). The fibroplasia caused by overexpression of TGFβ in the prostate was characterized by inflammation of the nerves and vessels, collapsed acini, breach of epithelial wall, and falloff of the epithelial cells into the ducts. The fibroplasia in the ERβ^crispr−/− mice sometimes filled the ducts blocking movement of secretions and causing enormously distended ducts. We have previously shown that ERβ regulates the inhibin wing of TGFβ signaling and, in the absence of ERβ, there is unrestrained activation of the activating wing of the TGF signaling pathway. In aging ERβ^OS−/− mice this led to granulosa cell tumors (24). Remarkably, the fibroplasia and stromal overgrowth were not dependent upon androgen signaling since they remained when androgen signaling was down-regulated in the 18-mo-old ERβ^crispr−/− mice.

Inflammation plays a key role in growth, invasiveness, and metastasis of PCa (25) and, as PCa progresses, NFκB promotes tumor invasion and metastasis (9). ERβ is a repressor of the master regulator of the immune system (26) and the main mediator of inflammation NFκB (27). Inflammation in the ERβ−/− mouse was reported very early as a marked phenotype in the characterization of the ER^OS−/− mouse prostate (6).

Although one cannot extrapolate from mice to humans, particularly in terms of regulation of gene expression, several clinical studies have shown that ERβ is reduced in early stages of PCa and reemerges in metastatic PCa (28–32). The clinical implication of the mouse findings is that ERβ agonists may be used in prevention of progression of PCa of low Gleason Grade to higher grades. However, since expression of ERβ is lost as PCa progresses above Gleason grade 3+3 (13, 30), ERβ agonists should be most effective in early stages of PCa. Men with cancers at or below a Gleason grade 3+3 are not treated with pharmaceuticals but are carefully monitored for signs of progression to higher grades. When cancers are driven by hormones, the standard clinical treatment approach is blocking the action of the hormone with hormone antagonists. Although very effective in the short term, what can emerge from this treatment is a cancer that proliferates in the absence of hormones (33). One of the mechanisms through which this hormone resistance occurs is emergence of cells in which the receptor is mutated and no longer needs hormones for activation (33, 34). If instead of a receptor antagonist, patients are given an ERβ agonist, expression and transcriptional activity of the receptor will be repressed whether the affinity of the receptor is activated by hormones. The site of action of ERβ agonists is at the promoter of the AR, not at its ligand binding domain. Thus, ERβ agonists offer a truly alternative approach to present pharmaceuticals that require binding to the ligand binding pocket of the receptor.

If ERβ reemerges in metastatic PCa as has been reported (29, 35), then ERβ agonists should be of use in treatment of CRPCa. The situation in breast cancer is different. In metastatic breast cancer, there is expression of ERα mutants (36, 37), which can make the cancer resistant to ERα antagonists. Since there is no ERα expressed in triple-negative breast cancer (TNBC), it is not yet known what the target of ERβ is, nor is it known whether ERβ is a driver of cancer in TNBC. In vitro studies with TNBC cell lines have shown that ERβ prevents invasiveness but does not affect proliferation (38–40). Studies with TNBC cell lines showed
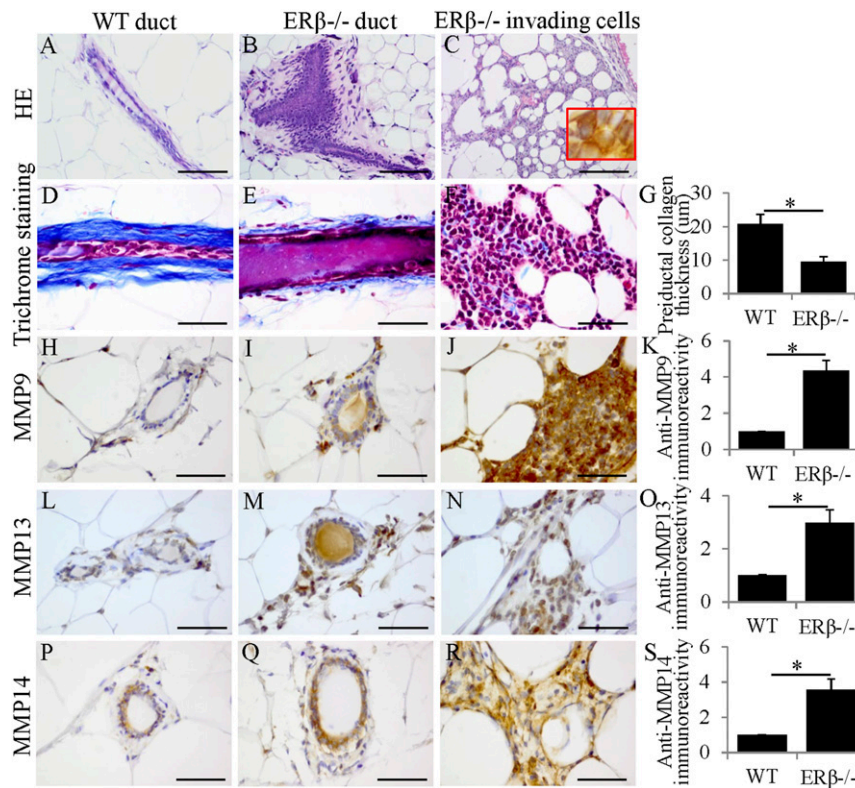
Fig. 9. Epithelial hyperplasia, invading cells, reduced collagen, and up-regulation of MMPs in MG of 6-mo-old ERβ[crispr−/−] female mouse. (*A*) HE staining shows normal duct of WT mouse MG. Epithelial hyperplasia in duct of ERβ[crispr−/−] mouse (*B*) and epithelial cells invading in the mammary fat pad, *Inset* shows invading cells were Ck14-positive (*C*). (*D*) Trichrome staining revealed a thick collagen layer surrounding the ducts of WT mice. (*E*) In the ERβ[crispr−/−] mouse, the collagen layer is very thin and the fibers are fragmented. (*F*) There is also very little collagen surrounding the epithelial cells invading the fat pad. (*G*) The difference in the width of the collagen layer surrounding the ducts is significant (*$P < 0.05$). Compared to WT mice, there is a marked induction in the expression of several MMPs. MMP9 with strong induction in adipocytes and invading cells (*H–K*); MMP13 induction in fibroblasts (*L–O*); MMP14 induction in epithelial cells and stroma (*P–S*). (Scale bars: *A–C*, 200 μm; *D–F*, *H–J*, *L–N*, and *P–R*, 50 μm.)

that ERβ can affect invasiveness by secretion of cystatins (41) and can increase innate immunity (42).

If in humans, ERβ agonists affect stromal, endothelial, and immune cells to alter the environment, prevent invasiveness, and increase activity of the immune system, they could be very useful clinically in treatment of PCa and TNBC. What remains to be done is to knock in ERβ in specific cells in the ERβ[crispr−/−] mouse so that the ERβ-target cells in the VP and MG can be precisely defined.

Materials and Methods

Materials, Animals, and Tissue Preparations. In this study, 6-mo, 8-mo, 10-mo, 13-mo, and 18-mo-old ERβ[crispr−/−] and age-matched WT male and female mice, C57BL/6 WT mice were used for experiments. The ERβ agonist, LY3201, (3aS, 4R, 9bR)-2, 2-difluoro-4-(4-hydroxyphenyl)-3, 3a, 4, 9b-tetrahydro-¹H-cyclopenta[c] chromen-8-ol (CAS 787621-78-7), was a gift from Eli Lilly. The mouse studies were approved by the Stockholm South ethical review board and the local Animal Experimentation Ethics Committee for animal experimentation (University of Houston animal protocol 09-036). All experimental protocols were adhered to the NIH Guidelines for the Care and Use of Laboratory Animals (43). Effort was made to minimize the number of animals used and their suffering. LY3201 treatment was similar to what we reported previously (19). Briefly, 10 2-mo-old and 10 6-mo-old C57BL/6 male mice were divided randomly into the following two groups: (*i*) treated with vehicle (*n* = 5) and (*ii*) treated with LY3201 (*n* = 5). LY3201 was used as pellets (0.04 mg/d), which were made by Innovative Research of America and implanted on the lateral side of the neck between the ear and the shoulder. The mice were treated by inserting pellets (vehicle or LY3201) 7 d before killing. Mice were housed in a room of standard temperature (22 ± 1 °C) with a regular 12-h light, 12-h dark cycle and given free access to water. All mice were terminally anesthetized by CO_2 and transcardially perfused with

phosphate-buffered saline (PBS) followed by 4% paraformaldehyde (in 0.1 M PBS, pH 7.4). Prostates and mammary glands were dissected and postfixed in the same fixative overnight at 4 °C. After fixation, tissues were processed for paraffin sections (5 μm).

qPCR. Ovaries were freshly collected and DNA was extracted by using DNEasy kit reagent according to the manufacturer's protocol. cDNA was generated from 1 μg of total RNA by using GeneAmp RNA PCR reagents (PerkinElmer) with random hexamers according to the manufacturer's protocol in a final volume of 25 μL. PCR was done with high-fidelity Taq DNA polymerase (Fermentas) with the following primers: (5′-GCCAATCATCGCTTCTCTAT-3′ and 5′-CCCTCTTTGCTCTTACTGTCCTCT-3′).

Immunohistochemistry. The immunohistochemistry protocol was the same as was reported previously (19). Slides with 5-μm paraffin-embedded sections were dewaxed in xylene, rehydrated, and processed for antigen retrieval with 10 mM citrate buffer (pH 6.0) in a Lab Vision PT module (Thermo Scientific). The cooled sections were incubated in a buffer composed of 50% (vol/vol) methanol and 3% (vol/vol) H_2O_2 for 30 min to quench endogenous peroxidase and then unspecific binding was blocked by incubating the slides in 3% (wt/vol) bovine serum albumin (BSA) with 0.1% Nonidet P-40 in PBS for 1 h. Sections were then incubated with anti-ERβ (1:100; made in our laboratory), anti-Ki67 (1:2,000; Abcam), anti-P63 (1:1,000; Abcam), anti-DACH1 (1:1,000; Abcam), anti-PURα (1:100; Abcam), anti-ERα (1:100; Abcam), anti-PR(1:100; Abcam), anti-MMP9 (1:100; Santa Cruz Biotechnology), anti-MMP13 (1:100; Abcam), anti-MMP14 (1:100; Abcam) at 4 °C after blocking nonspecific binding in 3% BSA. BSA replaced primary antibodies in negative controls. After washing, sections were incubated with HRP polymer kit (Biocare Medical; GHP516) for 30 min at room temperature, followed by 3, 3-diaminobenzidine tetrahydrochloride as the chromogen. We stained every fifth slide from 25 consecutive slices i.e., five slices from each mouse. The ImageJ software was used to quantitate levels of immunoreactivity. For

statistical analysis of the experimental data, WT mice or vehicle-treated mice were used as standards.

Masson's Trichrome Staining. Sections were dewaxed in xylene, rehydrated and washed in distilled water, then refixed in Bouin's solution for 1 h at 56 °C. After rinsing with tap water, sections were stained in Weigert's iron hematoxylin working solution for 10 min. Sections were then rinsed in running warm tap water for 10 min followed by washing in distilled water. Sections were stained in Biebrich scarlet-acid fuchsin solution for 15 min then differentiated in phosphomolybdic-phosphotungstic acid solution for 15 min. Sections were transferred to aniline blue solution and stained for 10 min. After rinsing in distilled water and differentiation in 1% acetic acid solution for 5 min, sections were dehydrated and mounted.

Microarray Data Processing and Analysis. RNA quality was assessed using an Agilent 2200 TapeStation (RIN values 8.3–10). One hundred fifty nanograms of total RNA was prepared from VPs from three WT and three ERβ$^{crispr-/-}$ mice (all 13 mo old) using the RNeasy kit from Qiagen following manufacturer's instructions (Qiagen). The total RNA was used to prepare biotinylated cDNA according to the GeneChip WT Plus Reagent Kit labeling protocol (P/N 902281). Fragmented cDNA was hybridized to mouse Clariom D (MTA 1.0, covering >214,000 coding and noncoding transcripts variants) arrays (Affymetrix) and analysis was performed as described earlier (44). Genes were filtered for a minimum log$_2$ change of 1.5 or greater across the samples. Genes were identified as significantly changed if the P value was <0.05.

Serum levels of estradiol and androgen were measured in a single run by GC-MS/MS, as described previously (45).

Data Analysis. Data are expressed as mean ± SD; statistical comparisons were made by using a one-way ANOVA followed by Newman–Keuls post hoc test. $P < 0.05$ was considered to indicate statistical significance.

Data Availability Statement. Raw data are available on Figshare at https://figshare.com/articles/Prostste_WT_vs_ERb_KO_MTA1_array_zip/11831076.

1. G. G. Kuiper, E. Enmark, M. Pelto-Huikko, S. Nilsson, J. A. Gustafsson, Cloning of a novel receptor expressed in rat prostate and ovary. *Proc. Natl. Acad. Sci. U.S.A.* **93**, 5925–5930 (1996).
2. M. C. Antal, A. Krust, P. Chambon, M. Mark, Sterility and absence of histopathological defects in nonreproductive organs of a mouse ERbeta-null mutant. *Proc. Natl. Acad. Sci. U.S.A.* **105**, 2433–2438 (2008).
3. Z. Weihua, M. Warner, J. A. Gustafsson, Estrogen receptor beta in the prostate. *Mol. Cell. Endocrinol.* **193**, 1–5 (2002).
4. L. Wang, S. Andersson, M. Warner, J. A. Gustafsson, Estrogen receptor (ER)beta knockout mice reveal a role for ERbeta in migration of cortical neurons in the developing brain. *Proc. Natl. Acad. Sci. U.S.A.* **100**, 703–708 (2003).
5. L. Maneix et al., Estrogen receptor β exon 3-deleted mouse: The importance of non-ERE pathways in ERβ signaling. *Proc. Natl. Acad. Sci. U.S.A.* **112**, 5135–5140 (2015).
6. G. S. Prins et al., Estrogen imprinting of the developing prostate gland is mediated through stromal estrogen receptor alpha: Studies with alphaERKO and betaERKO mice. *Cancer Res.* **61**, 6089–6097 (2001).
7. J. A. Gustafsson, A. Strom, M. Warner, Update on ERbeta. *J. Steroid Biochem. Mol. Biol.* **191**, 105312 (2019).
8. P. J. Kushner et al., Estrogen receptor pathways to AP-1. *J. Steroid Biochem. Mol. Biol.* **74**, 311–317 (2000).
9. C. Zhao et al., Genome-wide mapping of estrogen receptor-beta-binding regions reveals extensive cross-talk with transcription factor activator protein-1. *Cancer Res.* **70**, 5174–5183 (2010).
10. A. Wolfe, S. Wu, Estrogen receptor-β in the gonadotropin-releasing hormone neuron. *Semin. Reprod. Med.* **30**, 23–31 (2012).
11. J. Inzunza et al., Ovarian wedge resection restores fertility in estrogen receptor beta knockout (ERbeta-/-) mice. *Proc. Natl. Acad. Sci. U.S.A.* **104**, 600–605 (2007).
12. J. H. Krege et al., Generation and reproductive phenotypes of mice lacking estrogen receptor beta. *Proc. Natl. Acad. Sci. U.S.A.* **95**, 15677–15682 (1998).
13. P. Mak et al., Prostate tumorigenesis induced by PTEN deletion involves estrogen receptor β repression. *Cell Rep.* **10**, 1982–1991 (2015).
14. B. H. Norman et al., Benzopyrans are selective estrogen receptor beta agonists with novel activity in models of benign prostatic hyperplasia. *J. Med. Chem.* **49**, 6155–6157 (2006).
15. T. I. Richardson et al., Benzopyrans as selective estrogen receptor beta agonists (SERBAs). Part 3: Synthesis of cyclopentanone and cyclohexanone intermediates for C-ring modification. *Bioorg. Med. Chem. Lett.* **17**, 4824–4828 (2007).
16. C. G. Roehrborn et al., Estrogen receptor beta agonist LY500307 fails to improve symptoms in men with enlarged prostate secondary to benign prostatic hypertrophy. *Prostate Cancer Prostatic Dis.* **18**, 43–48 (2015).
17. C. Förster et al., Involvement of estrogen receptor beta in terminal differentiation of mammary gland epithelium. *Proc. Natl. Acad. Sci. U.S.A.* **99**, 15578–15583 (2002).
18. D. Ferrucci, M. F. Biancardi, U. Nishan, R. Rosa-Ribeiro, H. F. Carvalho, Desquamation takes center stage at the origin of proliferative inflammatory atrophy, epithelial-mesenchymal transition, and stromal growth in benign prostate hyperplasia. *Cell Biol. Int.* **41**, 1265–1270 (2017).
19. W. F. Wu et al., Estrogen receptor β, a regulator of androgen receptor signaling in the mouse ventral prostate. *Proc. Natl. Acad. Sci. U.S.A.* **114**, E3816–E3822 (2017).
20. T. Inoue et al., Purine-rich element binding protein (PUR) alpha induces endoplasmic reticulum stress response, and cell differentiation pathways in prostate cancer cells. *Prostate* **69**, 861–873 (2009).
21. M. Larsen et al., Molecular cloning and expression of ps20 growth inhibitor. A novel WAP-type "four-disulfide core" domain protein expressed in smooth muscle. *J. Biol. Chem.* **273**, 4574–4584 (1998).
22. L. G. Wang et al., Androgen receptor overexpression in prostate cancer linked to Pur alpha loss from a novel repressor complex. *Cancer Res.* **68**, 2678–2688 (2008).
23. D. A. Barron et al., TGF-beta1 induces an age-dependent inflammation of nerve ganglia and fibroplasia in the prostate gland stroma of a novel transgenic mouse. *PLoS One* **5**, e13751 (2010).
24. X. Fan et al., Gonadotropin-positive pituitary tumors accompanied by ovarian tumors in aging female ERbeta-/- mice. *Proc. Natl. Acad. Sci. U.S.A.* **107**, 6453–6458 (2010).
25. A. Rani, P. Dasgupta, J. J. Murphy, Prostate cancer: The role of inflammation and chemokines. *Am. J. Pathol.* **189**, 2119–2137 (2019).
26. G. S. Prins, K. S. Korach, The role of estrogens and estrogen receptors in normal prostate growth and disease. *Steroids* **73**, 233–244 (2008).
27. P. Mak, J. Li, S. Samanta, A. M. Mercurio, ERβ regulation of NF-kB activation in prostate cancer is mediated by HIF-1. *Oncotarget* **6**, 40247–40254 (2015).
28. P. Christoforou, P. F. Christopoulos, M. Koutsilieris, The role of estrogen receptor β in prostate cancer. *Mol. Med.* **20**, 427–434 (2014).
29. J. S. Lai et al., Metastases of prostate cancer express estrogen receptor-beta. *Urology* **64**, 814–820 (2004).
30. A. Bardin, N. Boulle, G. Lazennec, F. Vignon, P. Pujol, Loss of ERbeta expression as a common step in estrogen-dependent tumor progression. *Endocr. Relat. Cancer* **11**, 537–551 (2004).
31. L. G. Horvath et al., Frequent loss of estrogen receptor-beta expression in prostate cancer. *Cancer Res.* **61**, 5331–5335 (2001).
32. H. Bonkhoff, Estrogen receptor signaling in prostate cancer: Implications for carcinogenesis and tumor progression. *Prostate* **78**, 2–10 (2018).
33. T. Karantanos et al., Understanding the mechanisms of androgen deprivation resistance in prostate cancer at the molecular level. *Eur. Urol.* **67**, 470–479 (2015).
34. A. Anantharaman, T. W. Friedlander, Targeting the androgen receptor in metastatic castrate-resistant prostate cancer: A review. *Urol. Oncol.* **34**, 356–367 (2016).
35. I. Leav et al., Comparative studies of the estrogen receptors beta and alpha and the androgen receptor in normal human prostate glands, dysplasia, and in primary and metastatic carcinoma. *Am. J. Pathol.* **159**, 79–92 (2001).
36. S. A. Fuqua, G. Gu, Y. Rechoum, Estrogen receptor (ER) α mutations in breast cancer: Hidden in plain sight. *Breast Cancer Res. Treat.* **144**, 11–19 (2014).
37. K. Merenbakh-Lamin et al., D538G mutation in estrogen receptor-α: A novel mechanism for acquired endocrine resistance in breast cancer. *Cancer Res.* **73**, 6856–6864 (2013).
38. O. Hinsche, R. Girgert, G. Emons, C. Gründker, Estrogen receptor β selective agonists reduce invasiveness of triple-negative breast cancer cells. *Int. J. Oncol.* **46**, 878–884 (2015).
39. N. Hamilton et al., Biologic roles of estrogen receptor-β and insulin-like growth factor-2 in triple-negative breast cancer. *BioMed Res. Int.* **2015**, 925703 (2015).
40. S. Schüler-Toprak et al., Agonists and knockdown of estrogen receptor β differentially affect invasion of triple-negative breast cancer cells in vitro. *BMC Cancer* **16**, 951 (2016).
41. J. M. Reese et al., ERβ-mediated induction of cystatins results in suppression of TGFβ signaling and inhibition of triple-negative breast cancer metastasis. *Proc. Natl. Acad. Sci. U.S.A.* **115**, E9580–E9589 (2018).
42. L. Zhao et al., Pharmacological activation of estrogen receptor beta augments innate immunity to suppress cancer metastasis. *Proc. Natl. Acad. Sci. U.S.A.* **115**, E3673–E3681 (2018).
43. National Research Council, *Guide for the Care and Use of Laboratory Animals* (National Academies Press, Washington, DC, ed. 8, 2011).
44. M. K. Varshney et al., Role of estrogen receptor beta in neural differentiation of mouse embryonic stem cells. *Proc. Natl. Acad. Sci. U.S.A.* **114**, E10428–E10437 (2017).
45. C. Ohlsson et al.; EMAS Study Group, Comparisons of immunoassay and mass spectrometry measurements of serum estradiol levels and their influence on clinical association studies in men. *J. Clin. Endocrinol. Metab.* **98**, E1097–E1102 (2013).

MEDICAL SCIENCES